Journal of
Synchrotron Radiation

ISSN 0909-0495

Received 4 February 2009
Accepted 27 August 2009

Combined high pressure and heavy-ion irradiation: a novel approach

Maik Lang,[a] Fuxiang Zhang,[a] Jie Lian,[a,b] Christina Trautmann,[c] Reinhard Neumann[c] and Rodney C. Ewing[a]*

[a]Department of Geological Sciences and Department of Materials Science and Engineering, University of Michigan, 1100 North University Avenue, Ann Arbor, MI 48109-1005, USA, [b]Department of Mechanical, Aerospace and Nuclear Engineering, Rensselaer Polytechnic Institute, Troy, NY 12180, USA, and [c]GSI Helmholtzzentrum für Schwerionenforschung, Planckstr. 1, 64291 Darmstadt, Germany. E-mail: rodewing@umich.edu

Swift heavy-ion irradiations of a wide variety of materials have been used to modify and manipulate the properties of solids at the nanoscale. Recently, these high-energy irradiations have been successfully combined with high-pressure experiments. Based on results obtained for zircon ($ZrSiO_4$), this paper introduces this new experimental approach involving diamond anvil cells and large ion-accelerator facilities. This technique provides a wide spectrum of geoscience applications from nanoscale simulations of fission-track formation under crustal conditions to phase transitions of radiation-damaged minerals resulting from meteorite impact.

Keywords: zircon; reidite; high pressure; phase transitions; radiation damage; ion beams; nanocrystals.

1. Introduction

During the past few years there has been an increased interest in the response of materials to the extreme conditions of pressure, temperature and high-energy radiation fields. In a recently developed approach, these experimental environments have been, for the first time, combined simultaneously (Glasmacher *et al.*, 2006). This has been achieved by injecting relativistic ions from one of the world's largest accelerator facilities (GSI, Helmholtz Centre for Heavy Ion Research, Darmstadt, Germany) through a diamond anvil of a high-pressure cell into a pressurized target. First results showed that the combination of swift heavy ions and high pressure triggers dramatic material modifications that are not observed with the application of only pressure or only ion irradiation (Glasmacher *et al.*, 2006). By manipulating pressurized solids at the nanoscale, this technique has interesting applications in materials research; however, pressure, temperature and ion irradiations also provide a simulation of specific geological conditions. High-pressure and temperature experiments have aimed at reproducing the extreme conditions of Earth's interior in order to better understand material properties and quantify geodynamic processes. Many minerals that are exposed in natural environments to pressure and temperature (*e.g.* zircon) can incorporate and retain up to a few wt% uranium and thorium. Their decay over time leads to the accumulation of damage in the crystal structure (Ewing *et al.*, 2003; Weber *et al.*, 1994). Up to now, almost no information has been available on the interplay of this radiation damage and high-pressure and temperature regimes (Glasmacher *et al.*, 2006; Trachenko *et al.*, 2007; Liu *et al.*, 2008; Nasdala *et al.*, 2008). How does structural damage evolve in pressurized and heated materials? In contrast, what is the high-pressure response of minerals that have accumulated significant amounts of radiation damage?

This paper illustrates that ion-beam irradiations coupled with diamond anvil cells (DACs) is a suitable approach to simulate the combined environments of high pressure, temperature and radiation damage. A set of experiments have been completed for zircon that investigated fission-track formation within Earth's crust and the phase stability of pre-damaged zircon upon a high-pressure event (Lang, Lian *et al.*, 2008; Lang, Zhang *et al.*, 2008).

The spontaneous fission of ^{238}U produces energetic fragments, which induce narrow (diameter $\sim$5 nm) cylindrical zones of highly damaged zircon, the so-called fission tracks (Fleischer *et al.*, 1975; Wagner & Van den haute, 1992). Under elevated temperatures, these tracks fade by changing their number and length distribution, as revealed by chemical etching. This mechanism has been used for fission-track dating to infer the thermal history of geological samples (Wagner & Van den haute, 1992; Tagami & O'Sullivan, 2005). While temperature and pressure have been simulated separately, the combined effects of both parameters on the fission-track formation process have not been accessible up to now. Testing the influence of pressure and temperature is important, because zircon samples that are retained for some time within Earth's crust (*e.g.* in subduction zones) are exposed to both

environments. The track-size distribution is the most crucial parameter used to constrain the age and thermal history of a rock; thus, any pressure effects on fission tracks, *e.g.* a pressure-induced size variation, has major implications for the dating technique. We have simulated the formation of fission tracks under geologically relevant conditions by using relativistic ion projectiles to induce tracks in pressurized and heated zircon. The influence of crustal pressure on track formation was studied by comparison with a similar radiation damage process under ambient conditions.

Zircon exhibits an anomalous phase transformation at high pressure leading to a 10% denser phase, reidite, with the scheelite structure (Glass & Liu, 2001; Glass *et al.*, 2002; Gucsik *et al.*, 2004; Knittle & Williams, 1993; Kusaba *et al.*, 1985; Leroux *et al.*, 1999; Liu, 1979; Ono *et al.*, 2004; van Westrenen *et al.*, 2004). At elevated temperatures (~1400 K), reidite begins to form at pressures above ~10 GPa (Ono *et al.*, 2004). Owing to hampered kinetics, the critical pressure at room temperature has to be significantly overstepped in excess of 20 GPa (Knittle & Williams, 1993; van Westrenen *et al.*, 2004). Above this threshold, the transformation takes place gradually, with both phases coexisting, up to pressures of 30 to 40 GPa (Gucsik *et al.*, 2004; van Westrenen *et al.*, 2004). However, once the scheelite-structured phase is formed, it persists after pressure release and does not revert to zircon. Recently, metastable reidite was found in naturally occurring shock-metamorphosed zircon in the vicinity of a meteorite impact structure (Glass & Liu, 2001; Glass *et al.*, 2002). Thus, the zircon–reidite phase relation at elevated pressures has been considered as a peak-pressure indicator of such impact events (Glass & Liu, 2001; Kusaba *et al.*, 1985; Leroux *et al.*, 1999). The question of whether accumulated structural damage owing to radioactive decay may modify this phase transition has never been addressed. Here, we report experiments that investigate the effects of ion-beam-induced damage prior to a high-pressure event.

2. Experimental procedure

The simulation of fission tracks at crustal pressures and temperatures requires *in situ* irradiations of heated and pressurized zircon. A hydrothermal DAC of the Merrill–Bassett type (Merrill & Bassett, 1974) (see Fig. 1) was used to create pressure by squeezing two opposing diamond anvils against the sample chamber with an aperture (diameter ~0.5 mm) drilled in a steel gasket and filled with distilled water as the pressure-transmitting medium. The pressure was controlled by measuring laser-induced fluorescence of several small ruby grains distributed throughout the sample chamber (Mao *et al.*, 1986). Temperature was maintained by means of molybdenum heating wires wrapped around each diamond, and chromel–alumel thermocouples were placed close to the two anvil tips. A single-crystalline sample of zircon, ~300 µm in diameter and ~40 µm thick, was inserted into the DAC, and a pressure of approximately 7.5 kbar was applied. Shortly before the irradiation, the temperature was adjusted to 523 K (for about 1 h). The DAC was positioned at the beamline of cave A at the

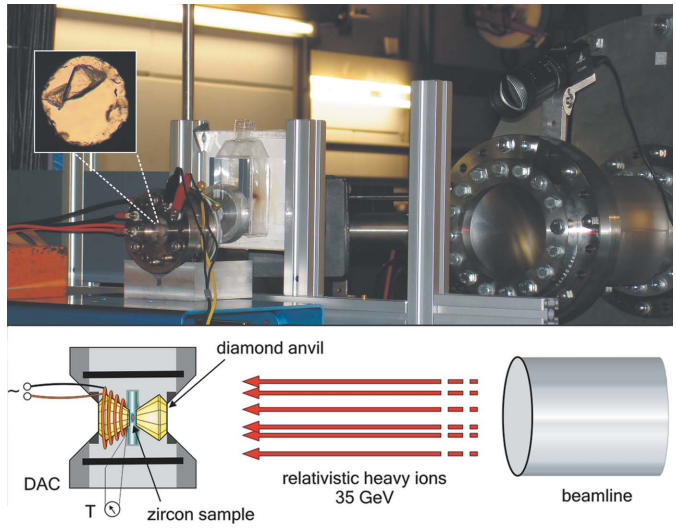

Figure 1
Photograph (top) and schematic illustration (bottom) of the irradiation experiment for exposing pressurized heated samples to a beam of relativistic heavy ions (Lang, Lian *et al.*, 2008). The small sample (300 µm in diameter and 40 µm thick) is enclosed in the diamond anvil cell (DAC). The inset displays the optical micrograph of a zircon crystal in the DAC. For the irradiation, the DAC is placed in air, 45 cm behind the beamline window. The schematic (not to scale) shows details of the DAC, including the resistance heating coil (only shown for one anvil).

heavy-ion synchrotron (SIS) of GSI (Fig. 1) and exposed to ^{208}Pb ions accelerated to relativistic energies of about 35 GeV. The ion beam, as delivered by the SIS, is pulsed (pulse length > 50 ms, rate ~1 Hz) and has a spot size of ~0.3 cm^2. In order to be able to image individual ion tracks, the fluence was limited to about 5×10^{10} ions cm^{-2}. The beam traverses the first 1.5 mm-thick diamond anvil and is slowed down to about 10 GeV as it reaches the pressurized zircon specimen (Lang *et al.*, 2005; SRIM, 2006). This reduced energy is sufficient that the ions completely pass through the sample and induce tracks. After irradiation and cooling, the DAC pressure was released and a crushed powder of the sample was inspected by means of transmission electron microscopy (TEM). For comparison, a zircon reference sample was irradiated at room temperature and ambient pressure, under the same ion-beam conditions.

For phase-transition studies on pre-damaged samples, the irradiation experiments were performed *ex situ*, *i.e.* the material was not simultaneously but subsequently exposed to ions and pressure. In a first step, a millimeter-sized synthetic single-crystalline sample of zircon was heavily damaged by a swift heavy-ion bombardment. Since a long ion range was not required (ions need not traverse a diamond anvil), the irradiation experiment was performed at the UNILAC accelerator of GSI. The polished 30 µm thin sample was entirely exposed to a defocused centimeter-sized 1.47 GeV ^{132}Xe beam with a calculated penetration depth of about 60 µm, *i.e.* the ions completely penetrated the sample (SRIM, 2006). In order to substantially damage the crystalline zircon structure, a fluence of 5×10^{12} ions cm^{-2} was applied (track-overlap regime). The irradiated sample was crushed between two glass plates and a small amount of powder (typical grain size of

several micrometers) was mounted into a symmetric Mao-type DAC, with a 16:3:1 mixture of methanol, ethanol and H_2O as the pressure-transmitting medium. Pressures up to 37 GPa at room temperature were adjusted by laser-induced ruby fluorescence (Mao *et al.*, 1986). The zircon structure was monitored under compression with a focus on the onset of the transformation to reidite by means of *in situ* synchrotron X-ray diffraction measurements (XRD) performed at the X17C beamline of the National Synchrotron Light Source at Brookhaven National Laboratory. Powder XRD with a monoenergetic beam of 30.5 keV and a spot size of ~25 μm was applied under increasing compression. Additionally, Raman spectroscopy measurements and TEM were completed on the quenched sample at 1 bar. For comparison, an unirradiated reference zircon was pressurized and analyzed under the same conditions.

3. Results

3.1. Fission tracks simulated at crustal pressures and temperatures

TEM images of heavy-ion tracks in zircon irradiated at ambient (Figs. 2*a*,2*b*) and at elevated pressure/temperature conditions (Fig. 2*c*,2*d*) were obtained. The tracks appear as cylindrical damage trails a few nanometers in diameter, as has been observed in previous TEM studies of natural fission tracks (Silk & Barnes, 1959; Chadderton *et al.*, 1966; Yada *et al.*, 1987), as well as artificial ion tracks (Bursill & Braunshausen, 1990). High-resolution images (Fig. 2*b*) clearly reveal the damage of the lattice structure within a track diameter of about 5 nm. For each sample, the diameter of 125 tracks was measured by visually estimating the position of the parallel boundaries between the track with a large aspect ratio (as shown in Fig. 2*d*) and the undamaged matrix. This yields a mean value ($\pm 1\sigma$) of the amorphous track diameter of 5.2 ± 0.5 nm and 5.4 ± 0.4 nm for zircon at ambient as well as at elevated pressure and temperature.

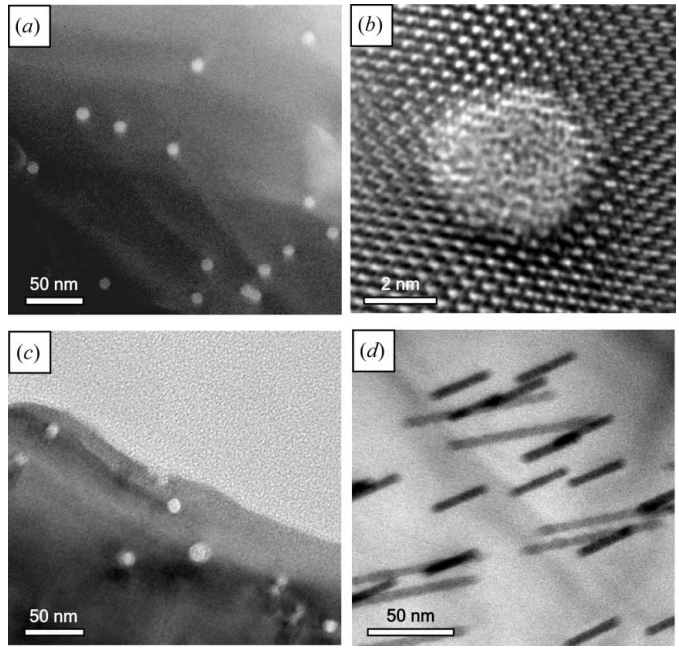

Figure 2
TEM images of zircon after exposure to 10 GeV Pb ions for a fluence of 5×10^{10} ions cm^{-2} (Lang, Lian *et al.*, 2008): (*a*, *b*) reference sample irradiated at room temperature and ambient pressure; (*c*, *d*) sample pressurized (7.5 kbar) and heated (523 K). (*a*, *c*) Bright-field micrographs of cross sections, (*d*) projections of tracks and (*b*) high-resolution image give evidence of the amorphous damage structure of the tracks.

3.2. Irradiation-induced stabilization at high pressure

Diffraction patterns up to 25.5 GPa on the unirradiated sample reveal only the zircon peaks (Fig. 3*a*). At pressures in excess of 26.5 GPa, new peaks characteristic of reidite are evident, and their intensities increase with increasing pressure (van Westrenen *et al.*, 2004). Thus, the unirradiated sample shows the phase transformation to reidite typical of zircon, although the pressure was 3–6 GPa higher than previously reported (Knittle & Williams, 1993; van Westrenen *et al.*, 2004). Similar pressure deviations have been attributed to compositional variations of different zircons (van Westrenen *et al.*, 2004, 2005) and may also be related to differential stress in the pressure chamber. At the maximum pressure of 37 GPa, the transformation to

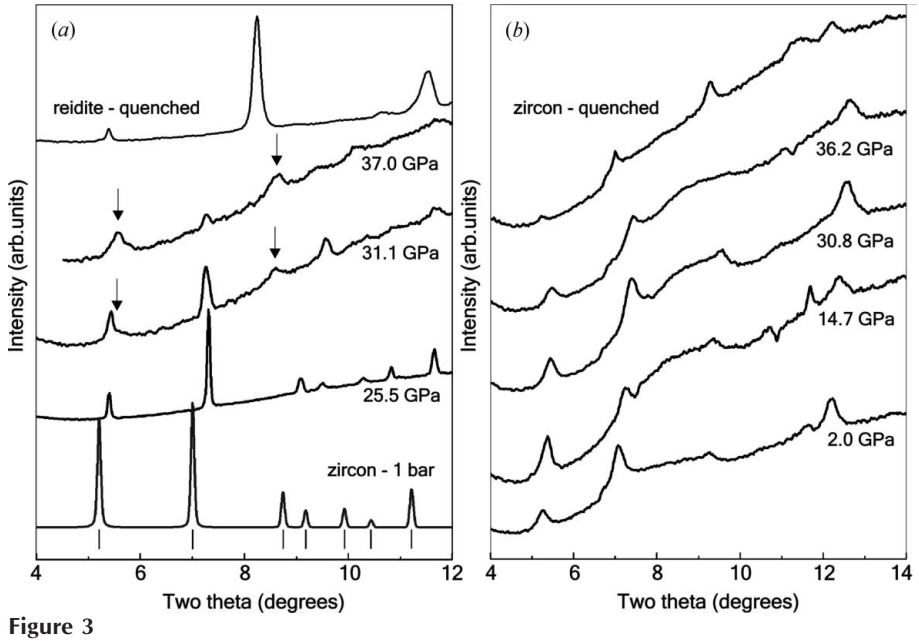

Figure 3
XRD data of zircon pressurized in diamond anvil cells (*a*) unirradiated and (*b*) irradiated with 1.47 GeV Xe ions of fluence 5×10^{12} cm^{-2} (Lang, Zhang *et al.*, 2008). (*a*) The undamaged zircon gradually transformed to reidite above 25.5 GPa, as indicated by new peaks (arrows); the sample quenched from 37 GPa showed only reidite diffraction peaks. The vertical bars indicate the diffraction-peak positions of the zircon structure. (*b*) The irradiated specimen showed no phase transition up to 36.2 GPa; the quenched sample exhibited only typical zircon diffraction peaks.

reidite was almost complete in the unirradiated sample, and the sample quenched to 1 bar exhibited for most part the diffraction maxima of reidite (Fig. 3*a*). In contrast, XRD analysis of the ion-irradiated zircon (pressurized and quenched) showed no obvious evidence of a pressure-induced transformation to reidite, even up to 36.2 GPa (Fig. 3*b*). The broad peak-structure, evident over the whole pressure range, is not related to the high-pressure phase, but is typical of radiation-damaged zircon (Ríos *et al.*, 2000; Ríos & Boffa-Ballaran, 2003).

Raman results are consistent with XRD analysis. Spectra of the unirradiated sample after compression (Fig. 4*a*) reveal an almost complete zircon–reidite transformation. The spectrum is dominated by peaks typical of reidite (Gucsik *et al.*, 2004), but also show the presence of some zircon remnants (indicated by its SiO_4 antisymmetric stretching mode at about 1000 cm^{-1}). This is in agreement with earlier reports showing that zircon can coexist with reidite, even though XRD results suggested a complete conversion to reidite at the highest pressure (van Westrenen *et al.*, 2004). In contrast to the results for the unirradiated zircon, we found no evidence of a substantial transformation to the high-pressure phase in the pre-irradiated zircon, after pressure release (Fig. 4*b*). Only a few sample spots exhibited small traces of reidite as evidenced by some of its vibration modes. For the most part, the Raman spectra recorded before (not shown here) and after compression are very similar, which is consistent with XRD results. The increased peak width, the small peak shifts and the high background of the irradiated sample can be explained as being due to radiation effects (Gucsik *et al.*, 2004).

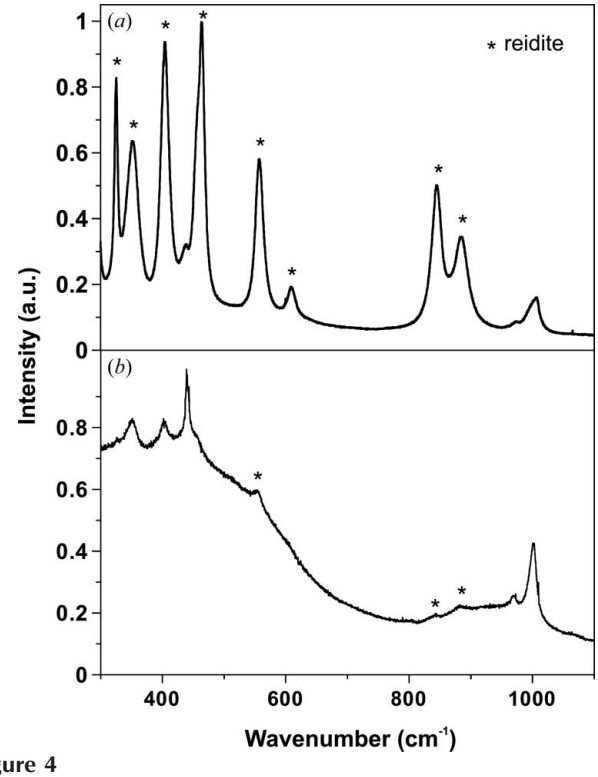

Figure 4
Raman spectra of (*a*) unirradiated and (*b*) ion-irradiated zircon after applying a pressure up to 37 GPa followed by pressure release (Lang, Zhang *et al.*, 2008). (*a*) Only traces of zircon were observed in the sample without irradiation, revealing an almost complete transformation to reidite. (*b*) Only traces of reidite were observed in the irradiated sample indicating a significant increase in zircon stability. The expected reidite Raman modes are labeled by asterisks (*).

4. Discussion

The selection of the experimental conditions for the fission-track simulation experiment was based on a consideration of the geologic conditions of greatest interest. An average geothermal gradient for the continental crust is about 25 K km^{-1} (Ehlers, 2005). Fission tracks in zircon that are typically used for geochronology and thermochronology are formed over a temperature regime not exceeding about 620 K and at depths less than ~14 km, which corresponds to a pressure up to 5 kbar. However, in some exceptional cases, fission-track-dated samples originate from even more 'extreme' geologic pressure conditions, such as from the high-pressure low-temperature rocks characteristic of subduction zones. Thus, by using a combination of 7.5 kbar and 623 K, the experimental conditions are typical of those described in classic subduction zones, *e.g.* Crete (Brix *et al.*, 2002). The mean track diameters for the ambient and elevated temperature/pressure samples differ by 0.2 ± 0.07 nm (the error resulting from the standard deviations of the mean values), which suggests that there are two distinct populations. The slightly larger size of the tracks at elevated pressure can be understood in terms of the increased efficiency of the damage process in a strained crystal lattice (Gibbons, 1972; Weber, 2000; Benyagoub, 2005). However, this probably will not affect the dimensions of etched tracks as utilized for fission-track dating.

The pressurization of pre-irradiated zircon demonstrated that the accumulation of structural damage modifies the zircon–reidite transformation at high pressures. Both synchrotron XRD and Raman scattering independently confirmed that the irradiation with swift heavy ions substantially increases the stability of zircon at high pressures. TEM analysis of the irradiated sample prior to the application of pressure revealed that the 1.47 GeV xenon ions had heavily damaged the crystal structure of zircon inducing cylindrical amorphous domains and fragmentation into nanocrystals (as a result of track-overlap at high fluences). Materials consisting of such nanometer-sized crystals may follow different thermodynamic pathways under pressure, as compared with that of the bulk samples (San-Miguel, 2006). For some solids, the critical pressure of a phase transition under compression is lower for nanocrystals (Wang *et al.*, 2001). However, it is generally observed that nanoparticles have a broader stability range (San-Miguel, 2006; Tolbert *et al.*, 1996). This behavior is mainly attributed to size effects of nanomaterials as reflected in a modified defect structure and a lack of nucleation sites (San-Miguel, 2006). An alternative explanation is based on shape changes that occur during phase transitions (Tolbert *et al.*, 1996). The zircon–reidite transition is characterized by a special displacive mechanism involving simple shearing, followed by small atomic adjustments (Kusaba *et al.*, 1986).

Owing to the size of the nanocrystalline 'islands' of zircon, such shearing could be ineffective in the irradiated sample. In contrast to bulk materials, pressure-induced local shearing could be relaxed in the nanometer-sized crystallites by means of a small rotation within the amorphous matrix. This behavior would explain the absence of reidite in the ion-irradiated sample under compression. However, it should be mentioned that other effects may contribute to an increased phase stability of pre-damaged zircon. Irradiation-induced defects in the nanocrystals and densification of the amorphous phase under pressure could also influence the energetics of the zircon–reidite transition.

5. Conclusions

We have presented a new and powerful experimental approach to simulate the interplay of structural damage and high-pressure/temperature environments. Fission-track formation was studied under well controlled pressure and temperature conditions that are typical of Earth's crust. For natural zircon irradiated at 7.5 ± 0.5 kbar and 523 ± 5 K, there was a minor diameter increase compared with tracks formed under ambient conditions. Further, the pressure-induced phase transition in pre-damaged zircon was investigated. For heavily irradiated zircon, only traces of reidite were found within a pressure range for which a non-irradiated sample was almost completely transformed to the scheelite-structured high-pressure phase. This increased stability at higher pressures is ascribed to radiation-induced nanoscale modifications. Critical pressure and temperature values of phase transitions can obviously be significantly changed by the microstructure that results from radiation damage. This is an important observation because high-pressure events experienced by natural zircons, which have accumulated radiation damage, may lead to an unexpectedly low reidite content.

The authors thank the organizing committee of the workshop 'Advances in High-Pressure Science Using Synchrotron X-rays' for their invitation to present our recent research activities on the combined effects of high pressure and ion irradiation. The authors gratefully acknowledge technical support from James Hinchcliff, Hans Keppler, Wendy Panero, Daniel Reaman, Dieter Schardt, Elko Schubert, Beatrice Schuster and Lars Stixrude. This paper has benefitted from technical reviews by Marin Clark, Todd Ehlers and Günther A. Wagner. This work was supported by the Office of Basic Energy Sciences, USDOE under DOE grant DE-FG02-97ER45656. The use of the National Synchrotron Light Source at X17C station is supported by NSF COMPRES EAR01-35554 and by US-DOE contract DE-AC02-10886. ML acknowledges support from the German Science Foundation DFG.

References

Benyagoub, A. (2005). *Phys. Rev. B*, **72**, 094114.
Brix, M. R., Stockhert, B., Seidel, E., Theye, T., Thomson, S. N. & Kuster, M. (2002). *Tectonophysics*, **349**, 309–326.
Bursill, L. A. & Braunshausen, G. (1990). *Philos. Mag. A*, **62**, 395–420.
Chadderton, L. T., Morgan, D. V., Torrens, I. McC. & Van Vliet, D. (1966). *Philos. Mag.* **13**, 185–195.
Ehlers, T. A. (2005). *Rev. Miner. Geochem.* **58**, 315–350.
Ewing, R. C., Meldrum, A., Wang, L.-M., Weber, W. J. & Corrales, L. R. (2003). *Rev. Miner. Geochem.* **53**, 387–425.
Fleischer, R. L., Price, P. B. & Walker, R. M. (1975). *Nuclear Tracks in Solids: Principles and Applications*, p. 605. Berkeley: University of California Press.
Gibbons, J. F. (1972). *Proc. IEEE*, **60**, 1062–1096.
Glasmacher, U. A., Lang, M., Keppler, H., Langenhorst, F., Neumann, R., Schardt, D., Trautmann, C. & Wagner, G. A. (2006). *Phys. Rev. Lett.* **96**, 195701.
Glass, B. P. & Liu, S. (2001). *Geology*, **29**, 371–373.
Glass, B. P., Liu, S. & Leavens, P. B. (2002). *Am. Mineral.* **87**, 562–565.
Gucsik, A., Zhang, M., Koeberl, C., Salje, E. K. H., Redfern, S. A. T. & Pruneda, J. M. (2004). *Mineral. Mag.* **68**, 801–811.
Knittle, E. & Williams, Q. (1993). *Am. Mineral.* **78**, 245–252.
Kusaba, K., Syono, Y., Kikuchi, M. & Fukuoka, K. (1985). *Earth Planet. Sci. Lett.* **72**, 433–439.
Kusaba, K., Yagi, T., Kikuchi, M. & Syono, Y. (1986). *J. Phys. Chem. Solids*, **47**, 675–679.
Lang, M., Glasmacher, U. A., Neumann, R., Schardt, D., Trautmann, C. & Wagner, G. A. (2005). *Appl. Phys. A*, **80**, 691–694.
Lang, M., Lian, J., Zhang, F. X., Hendriks, B. W. H., Trautmann, C., Neumann, R. & Ewing, R. C. (2008). *Earth Planet. Sci. Lett.* **274**, 355–358.
Lang, M., Zhang, F. X., Lian, J., Trautmann, C., Neumann, R. & Ewing, R. C. (2008). *Earth Planet. Sci. Lett.* **269**, 291–295.
Leroux, H., Reimold, W. U., Koeberl, C., Hornemann, U. & Doukhan, J.-C. (1999). *Earth Planet. Sci. Lett.* **169**, 291–301.
Liu, J., Glasmacher, U. A., Lang, M., Trautmann, C., Voss, K.-O., Neumann, R., Wagner, G. A. & Miletich, R. (2008). *J. Appl. Phys. A*, **91**, 17–22.
Liu, L.-G. (1979). *Earth Planet. Sci. Lett.* **44**, 390–396.
Mao, H.-K., Xu, J. & Bell, P. M. (1986). *Geophys. Res.* **91**, 4673–4676.
Merrill, L. & Bassett, W. A. (1974). *Rev. Sci. Instrum.* **45**, 290–294.
Nasdala, L., Miletich, R., Ruschel, K. & Váczy, T. (2008). *Phys. Chem. Miner.* **35**, 597–602.
Ono, S., Funakoshi, K., Nakajima, Y., Tange, Y. & Katsura, T. (2004). *Contrib. Mineral. Petrol.* **147**, 505–509.
Ríos, S. & Boffa-Ballaran, T. (2003). *J. Appl. Cryst.* **36**, 1006–1012.
Ríos, S., Salje, E. K. H., Zhang, M. & Ewing, R. C. (2000). *J. Phys. Condens. Matter*, **12**, 2401–2412.
San-Miguel, A. (2006). *Chem. Soc. Rev.* **35**, 876–889.
Silk, E. C. H. & Barnes, R. S. (1959). *Philos. Mag.* **4**, 970–971.
SRIM (2006). *SRIM 2006 – The Stopping and Range of Ions in Matter*, http://www.srim.org/SRIM/SRIM2006.htm.
Tagami, T. & O'Sullivan, P. B. (2005). *Rev. Miner. Geochem.* **58**, 19–47.
Tolbert, S. H., Herhold, A. B., Brus, L. E. & Alivisatos, A. P. (1996). *Phys. Rev. Lett.* **76**, 4384–4387.
Trachenko, K., Brazhkin, V. V., Tsiok, O. B., Dove, M. T. & Salje, E. K. H. (2007). *Phys. Rev. Lett.* **98**, 135502.
Van Westrenen, W., Frank, M. R., Fei, Y., Hanchar, J. M., Finch, R. J. & Zha, C.-S. (2005). *J. Am. Ceram. Soc.* **88**, 1345–1348.
Van Westrenen, W., Frank, M. R., Hanchar, J. M., Fei, Y., Finch, R. J. & Zha, C.-S. (2004). *Am. Mineral.* **89**, 197–203.
Wagner, G. A. & Van den haute, P. (1992). *Fission Track-Dating*, p. 285. Dordrecht: Kluwer Academic.
Wang, Z., Saxena, S. K., Pischedda, V., Liermann, H. P. & Zha, C. S. (2001). *Phys. Rev. B*, **64**, 012102.
Weber, W. J. (2000). *Nucl. Instrum. Methods Phys. Res. B*, **166–167**, 98–106.
Weber, W. J., Ewing, R. C. & Wang, L.-M. (1994). *J. Mater. Res.* **9**, 688–698.
Yada, K., Tanji, T. & Sunagawa, I. (1987). *Phys. Chem. Miner.* **14**, 197–204.